

# Improved Thermoelectric Behavior of Nanotube-Filled Polymer Composites with Poly(3,4-ethylenedioxothiophene) Poly(styrenesulfonate)

Dasaroyong Kim, Yeonseok Kim, Kyungwho Choi, Jaime C. Grunlan,\* and Choongho Yu\*

Department of Mechanical Engineering, Texas A&M University, College Station, Texas 77843

**T**hermoelectric systems are very effective in harvesting electricity from waste heat or heat sources with low temperature gradients relative to the environmental temperature.<sup>1,2</sup> Low temperature gradients are inadequate for power generation using conventional systems but are often present in the environment (e.g., solar and geothermal energy) or generated from various power generating or consuming systems. The simple leg-type structures, without moving parts, have significant advantages over conventional turbines, engines, and compressors. In addition, their high energy density (per unit weight and volume) is ideal for mobile power sources and distribution systems. This high power density and simple structure have attracted intense research effort toward improving thermoelectric efficiency. Despite significant efforts, there has been only marginal improvement in thermoelectric efficiency since the discovery of bismuth telluride alloys in 1960s.<sup>3</sup> Typical thermoelectric semiconductor materials are expensive and relatively difficult to process,<sup>4</sup> impeding their widespread use for energy conversion. As a result, it is very timely and necessary to investigate high power-density (or lightweight) and relatively economical thermoelectric materials.

In this regard, polymer nanocomposites are very attractive as they are light and generally require relatively simple manufacturing processes compared to semiconductor-based thermoelectrics. The poor thermal conductivity intrinsic to typical polymers is ideal for thermoelectrics because the thermoelectric figure of merit (*ZT*), which is a measure of thermoelectric energy conversion efficiency, is defined as

**ABSTRACT** The thermoelectric properties of carbon nanotube (CNT)-filled polymer composites can be enhanced by modifying junctions between CNTs using poly(3,4-ethylenedioxothiophene) poly(styrenesulfonate) (PEDOT:PSS), yielding high electrical conductivities (up to  $\sim 40000$  S/m) without significantly altering thermopower (or Seebeck coefficient). This is because PEDOT:PSS particles are decorated on the surface of CNTs, electrically connecting junctions between CNTs. On the other hand, thermal transport remains comparable to typical polymeric materials due to the dissimilar bonding and vibrational spectra between CNT and PEDOT:PSS. This behavior is very different from that of typical semiconductors whose thermoelectric properties are strongly correlated. The decoupled thermoelectric properties, which is ideal for developing better thermoelectric materials, are believed to be due to thermally disconnected and electrically connected contact junctions between CNTs. Carrier transport at the junction is found to be strongly dependent on the type and concentration of stabilizers. The crucial role of stabilizers was revealed by characterizing transport characteristics of composites synthesized by electrically conducting PEDOT:PSS and insulating gum Arabic (GA) with 1:1–1:4 weight ratios of CNT to stabilizers. The influence of composite synthesis temperature and CNT-type and concentration on thermoelectric properties has also been studied. Single-walled (SW) CNT-filled composites dried at room temperature followed by 80 °C exhibited the best thermoelectric performance in this study. The highest thermoelectric figure of merit (*ZT*) in this study is estimated to be  $\sim 0.02$  at room temperature, which is at least one order of magnitude higher than most polymers and higher than that of bulk Si. Further studies with various polymers and nanoparticles with high thermoelectric performance may result in economical, lightweight, and efficient polymer thermoelectric materials.

**KEYWORDS:** segregated network · carbon nanotube · polymer thermoelectrics · PEDOT:PSS · conducting polymer · stabilizer

$$ZT = \frac{S^2 \sigma T}{k} \quad (1)$$

where *S*,  $\sigma$ , *k*, and *T* are thermopower (or Seebeck coefficient), electrical conductivity, thermal conductivity, and absolute temperature, respectively.<sup>5</sup> Nevertheless, low electrical conductivity and thermopower have excluded polymers as feasible candidates in the past. With the addition of electrically conductive particles, the electrical conductivity of polymers can be brought into degenerate-semiconductor or metallic regimes. This conversion can be accomplished with a relatively low concentration of nanoparticles when a segregated

\*Address correspondence to  
chyu@tamu.edu,  
jgrunlan@tamu.edu.

Received for review October 4, 2009  
and accepted December 17, 2009.

Published online December 30, 2009.  
10.1021/nn9013577

© 2010 American Chemical Society

network is employed.<sup>6–9</sup> These networks can be created with a polymer emulsion, whose particles create excluded volume and essentially push particles into the interstitial space between them. This situation dramatically reduces the space available for the conductive particles to form networks, resulting in a significant enhancement of electrical conduction with a relatively small concentration of particles.<sup>6,10</sup>

In typical bulk semiconductors, thermoelectric properties are strongly correlated, making *ZT* enhancement very difficult. For example, an increase of electrical conductivity often accompanies a decrease of thermopower and an increase of thermal conductivity. Despite these trends in typical solids, our previous study with carbon nanotubes (CNTs) and poly(vinyl acetate) (PVAc) latex showed that it is possible to increase electrical conductivity and keep thermopower and thermal conductivity relatively constant.<sup>6</sup> This behavior is governed by electrically connected but thermally disconnected junctions between CNTs. A small energy barrier for electron transport at the junctions plays an important role in deterring low energy electron transport, making thermopower insensitive to the increase of electrical conductivity. The barrier for energy carrier transport across the junctions can be significantly altered by changing stabilizers that are necessary for dispersing and exfoliating CNTs,<sup>11,12</sup> which naturally form bundles due to van der Waals force between them. Highly entangled nanotubes are difficult to disperse in organic solvent or water without a stabilizer, resulting in disconnected or less-branched networks. Electron transport across junctions is influenced by interparticle distance, electronic states of CNTs, contact potential barriers, and electrostatic charges of CNTs and matrices,<sup>13,14</sup> which can be altered with stabilizing agents. There are several types of stabilizers that have been used to disperse nanotubes in polymers such as surfactants,<sup>15–18</sup> polymers,<sup>19–22</sup> biomolecules,<sup>23,24</sup> and inorganic nanoparticles.<sup>25,26</sup> Most dispersants are electrical insulators that hinder electron transport across the junctions. Recently, it was shown that an intrinsically conductive polymer, poly(3,4-ethylenedioxothiophene):poly(styrene sulfonate) (PEDOT:PSS), can effectively stabilize and disperse nanotubes in water,<sup>14</sup> thereby enhancing electrical conductivity by preventing settling and aggregation of CNTs. PEDOT:PSS has been widely used as an antistatic coating material, electrodes for capacitors or photodiodes, transparent electrodes for solar cells, and a hole transport layer for organic LED.<sup>21,27–30</sup> Its electrical conductivity can be greatly enhanced with solvent doping such as dimethyl sulfoxide (DMSO).<sup>27,31</sup>

In the present work, PEDOT:PSS, doped with DMSO, was used to disperse CNTs in water. Additionally, transport properties with electrically insulating gum arabic (GA) were also studied for comparison. The electrical conductivity of composites with PEDOT:PSS is much

higher than that of GA composites, and increases with higher CNT concentration or more PEDOT:PSS with respect to CNT wt %. Drying at an elevated temperature also results in an increase of electrical conductivity, but thermopower is relatively insensitive to the change. Replacing XM-grade CNTs (XM-CNTs) with purified single-walled carbon nanotubes (SWCNTs) shows two or three time increases in electrical conductivity with similar thermopowers. With high SWCNT concentration (35 wt %), the electrical conductivity was measured to be ~40000 S/m, which is more than 100 times higher than those of typical polymer composites<sup>13,32,33</sup> containing high nanotubes concentration (>10 wt %). The large enhancement in electrical properties did not significantly alter thermal conductivity from those of typical polymers (0.2–0.4 W/(m · K)). The following sections describe preparation, microstructures, and thermoelectric properties of CNT-polymer composites. The influence of type and concentration of stabilizers and drying condition on thermoelectric properties has been systematically studied. Finally, these experimental results would provide a pathway for improving the thermoelectric figure of merit of polymer nanocomposites.

## RESULTS AND DISCUSSION

Figure 1 panels a and b show schematics of CNTs dispersed by GA and PEDOT:PSS. Both dispersants exfoliate CNTs and modify their surfaces, making CNTs hydrophilic and thereby stabilized in water. Figure 1 panels c and d illustrate the formation of a segregated network during the drying of water-based polymer emulsions that occurs after addition of stabilized CNTs. Initially, the nanotubes and polymer particles are uniformly dispersed in water (left). During drying (water evaporation), the polymer particles push the nanotubes into interstitial spaces to form a segregated network (right). Table 1 summarizes six different sets (samples A–F) of polymer composites prepared for this study. The composite matrix is a copolymer latex containing vinyl acetate and ethylene. Because of the low glass transition temperature ( $T_g$ ) of this polymer emulsion (~15 °C), it is more flexible than the poly(vinyl acetate) homopolymer ( $T_g$  = 35 °C) that was used to make composites reported earlier.<sup>6</sup> XM-CNTs (Carbon Nanotechnologies, Inc.), which are a mixture of metallic and semi-conducting single-, double-, and triple-walled CNTs, were used as a low cost alternative to SWCNTs. Higher-quality SWCNTs were also used to achieve enhanced thermoelectric performance with the best recipe for XM-CNT filled composites.

For the first set of samples (A1–A6), six different XM-CNT concentrations, 2.1, 4.4, 6.9, 9.8, 12.5, and 15 wt % (with a fixed 1:4 weight ratio between CNTs and PEDOT:PSS) were used to study the influence of the filler concentration. The second set of samples (B1–B4) were synthesized to compare thermoelectric properties of composites made with electrically conducting PEDOT:

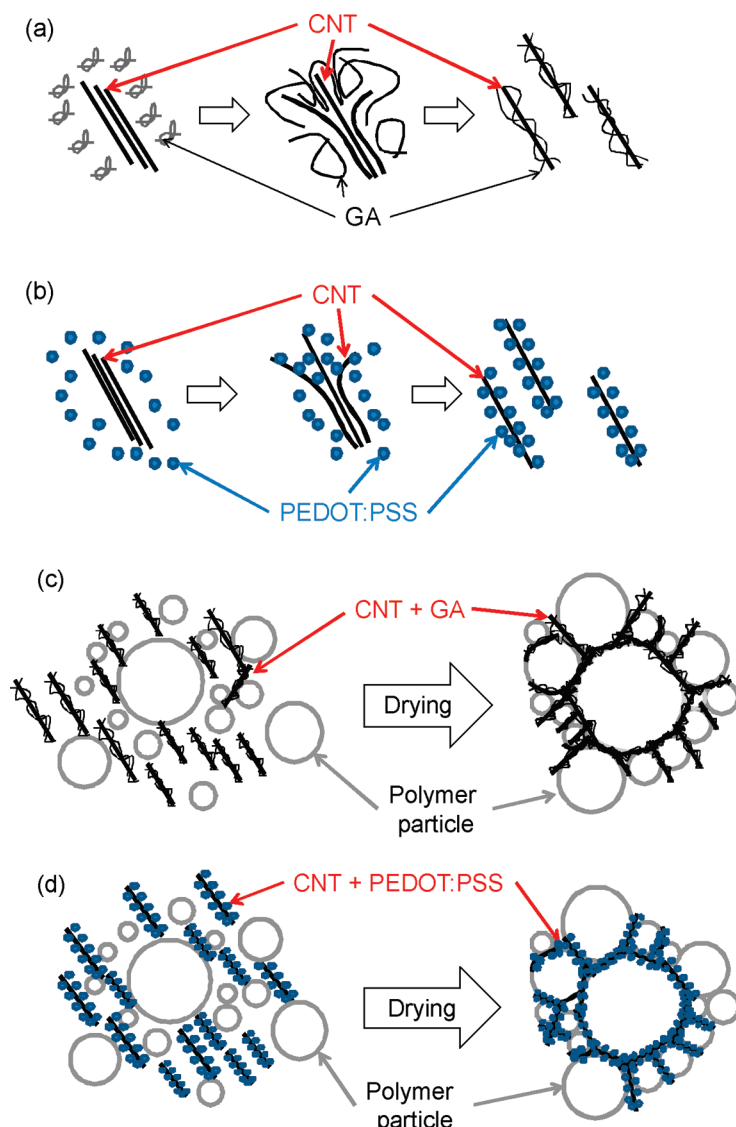


**Figure 1.** CNTs form a three-dimensional network along the surface of spherical emulsion particles. Panels **a** and **b** show schematics of CNTs dispersed by GA and PEDOT:PSS, respectively. Panels **c** and **d** show schematic illustrations of segregated-network formation before (left) and after (right) the drying of water-based polymer emulsions.

PSS and insulating GA stabilizers. The third set (C1–C4) uses four different weight ratios of CNTs to PEDOT:PSS (1:1, 1:2, 1:3, and 1:4). PEDOT:PSS concentration affects CNT dispersion and transport behavior at tube–tube junctions. Excessive PEDOT:PSS could also form a segregated network by itself. For the fourth set of samples (D1–D4), an elevated drying temperature (80 °C) was used. The high temperature removes excess dopant (DMSO) as well as strengthens the segregated network. The fifth and sixth sets of composites (E1–E3 and F1–F3) were dried at room temperature, followed by further drying at 80 °C. Samples E1–E3 show the influence of the mixed drying condition and PEDOT:PSS concentration at a high (20 wt %) CNT concentration. Substituting SWCNTs for XM-CNTs (samples F1–F3) further raises electrical conductivity, as discussed below.

Scanning electron micrographs (SEMs) shown in Figure 2 are the freeze-fractured cross sections of compos-

ites with different CNT concentrations (samples A2, A3, A5, and A6). PEDOT:PSS particles and CNTs are shown as bright dots and curved lines, respectively, in these images. The PEDOT:PSS particles are observed along the CNTs, which provides evidence for the affinity between these materials. At a concentration of 4.4 wt %, most CNTs are embedded within the polymer matrix, showing that the interaction between CNTs and the polymer matrix is strong. As the concentration increases up to 15 wt %, the network becomes thicker and many CNTs are pulled out from the matrix. An increase in porosity is also observed with higher CNT concentration. Microvoids start to form when the polymer emulsion can no longer envelop fillers due to high filler concentration. CNTs form networks upon drying, which are believed to serve as a barrier for emulsions to fully coalesce and fill these voids. These images, however, demonstrate that this low  $T_g$  composite is more homogeneous and able

**TABLE 1. CNT Concentration and Type, Stabilizer, Weight Ratio between CNT and Stabilizer, and Drying Temperature of the Samples Used for This Study**

sample number	CNT concentration (wt %)	CNT type <sup>a</sup>	stabilizer	CNT/stabilizer weight ratio	drying temperature
A1	2.1	XM	PEDOT:PSS	1:4	room temp
A2	4.4	XM	PEDOT:PSS	1:4	room temp
A3	6.9	XM	PEDOT:PSS	1:4	room temp
A4	9.8	XM	PEDOT:PSS	1:4	room temp
A5	12.5	XM	PEDOT:PSS	1:4	room temp
A6	15	XM	PEDOT:PSS	1:4	room temp
B1	2	XM	GA	1:4	room temp
B2	4	XM	GA	1:4	room temp
B3	6	XM	GA	1:4	room temp
B4	8	XM	GA	1:4	room temp
C1	9.8	XM	PEDOT:PSS	1:1	room temp
C2	9.8	XM	PEDOT:PSS	1:2	room temp
C3	9.8	XM	PEDOT:PSS	1:3	room temp
C4	9.8	XM	PEDOT:PSS	1:4	room temp
D1	9.8	XM	PEDOT:PSS	1:1	80 °C
D2	9.8	XM	PEDOT:PSS	1:2	80 °C
D3	9.8	XM	PEDOT:PSS	1:3	80 °C
D4	9.8	XM	PEDOT:PSS	1:4	80 °C
E1	9.8	XM	PEDOT:PSS	1:4	room temp and 80 °C
E2	20	XM	PEDOT:PSS	1:1	room temp and 80 °C
E3	20	XM	PEDOT:PSS	1:2	room temp and 80 °C
F1	20	SW	PEDOT:PSS	1:1	room temp and 80 °C
F2	20	SW	PEDOT:PSS	1:2	room temp and 80 °C
F3	35	SW	PEDOT:PSS	1:1	room temp and 80 °C

<sup>a</sup>XM and SW stand for XM-grade CNTs and SWCNTs, respectively.

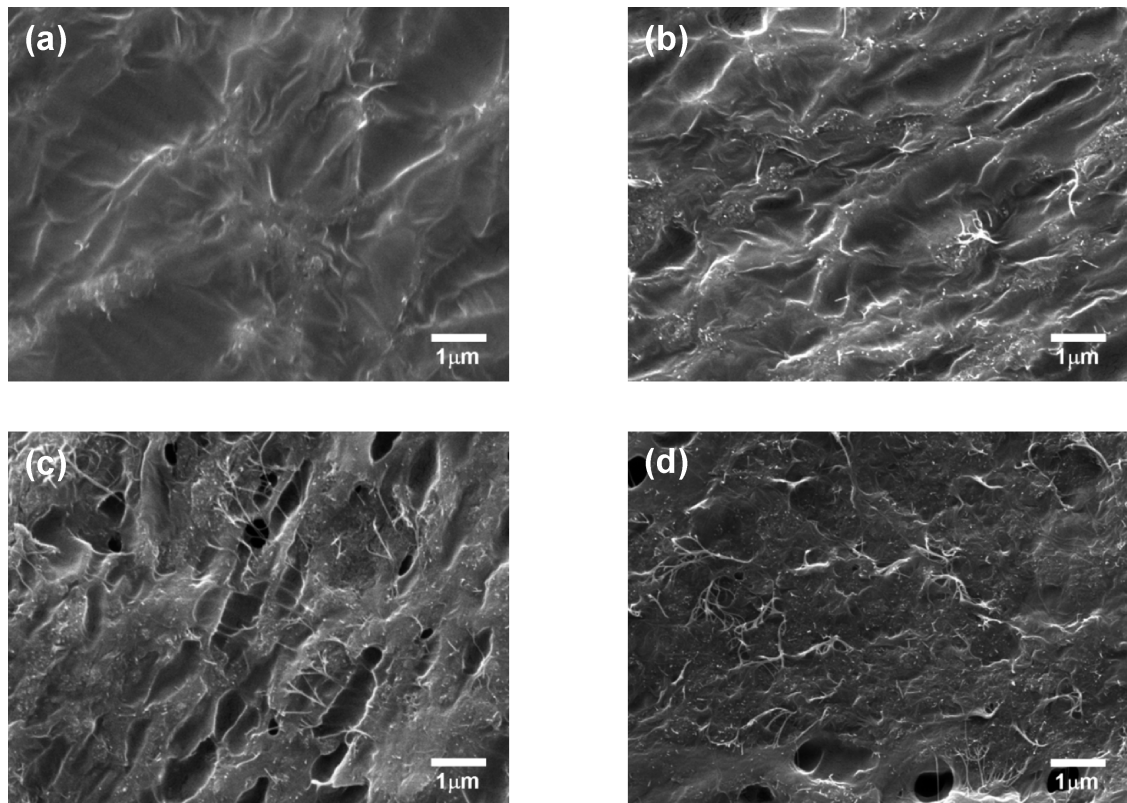


**Figure 2.** (a) Cross-section of a 4.4 wt % CNT composite (sample A2) after being freeze-fractured. Cross sections of 6.9, 12.5, and 15 wt % CNT composites (samples A3, A5, and A6, respectively) are shown in panels b, c, and d, respectively. The weight ratio of CNT to PEDOT is 1:4. All scale bars indicate 1  $\mu\text{m}$ . CNTs are spaghetti-like slender objects and PEDOT:PSS particles are protuberant spherical-shape objects (small dots) in the figures.

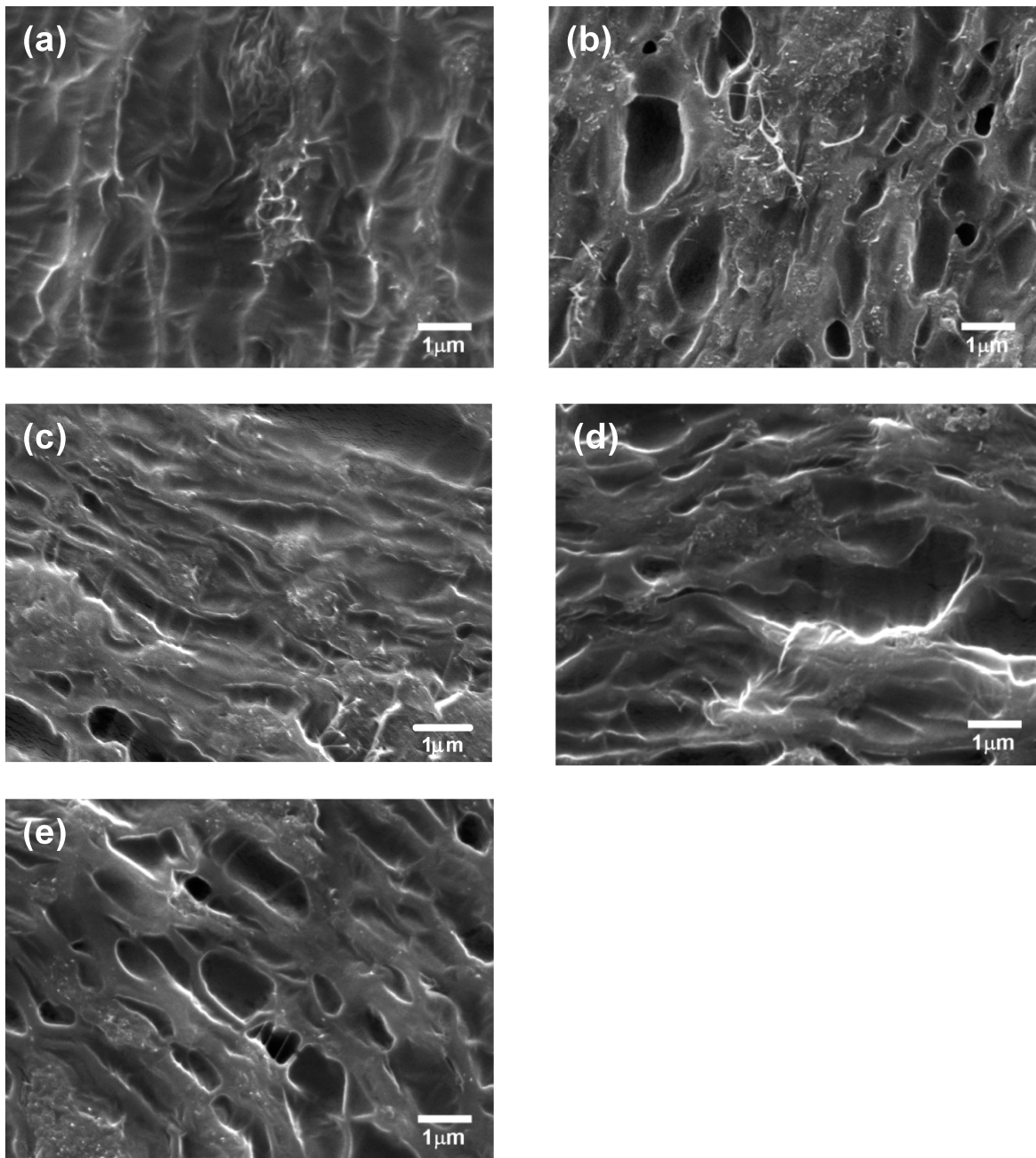


**Figure 3.** Freeze-fractured cross sections of 9.8 wt % CNT composites dried at room temperature with (a) 1:2 (sample C2) and (b) 1:4 (sample C4) ratio of CNT:(PEDOT:PSS). Cross sections of composites dried at 80 °C with a (c) 1:2 (sample D2) and (d) 1:4 (sample D4) ratio, and (e) dried at room temperature and subsequently 80 °C with 1:4 ratio (sample E1). All scale bars indicate 1  $\mu\text{m}$ . CNTs are spaghetti-like slender objects and PEDOT:PSS particles are protuberant spherical-shape objects (small dots) in the figures.

to incorporate more filler than composites made previously with a more rigid matrix.<sup>6,10</sup>

Figure 3 panels a and b (samples C2 and C4) show microstructures of room-temperature dried composites containing 9.8 wt % CNT with 1:2 and 1:4 weight ratios of CNT to PEDOT:PSS. According to these micrographs, it is not obvious how the amount of PEDOT:PSS affects the CNT dispersion because the images only show the surface of the samples. Nevertheless, the 1:4 composite clearly exhibits heavier aggregation of PEDOT:PSS particles with a higher level of porosity.

The aggregated and relatively rigid PEDOT:PSS is responsible for creating such voids.<sup>7</sup> Composites were also dried at an elevated temperature (80 °C) to examine the effect of drying temperature. The higher drying temperature resulted in a smoother surface and stronger interaction between CNTs and the matrix, especially for the 1:4 composite, as shown in Figure 3c,d (samples D2 and D4). Most of the CNTs are embedded in the polymer matrix without voids when the composites were dried at 80 °C. This improved structure is largely due to a decreased modulus of the emulsion particles

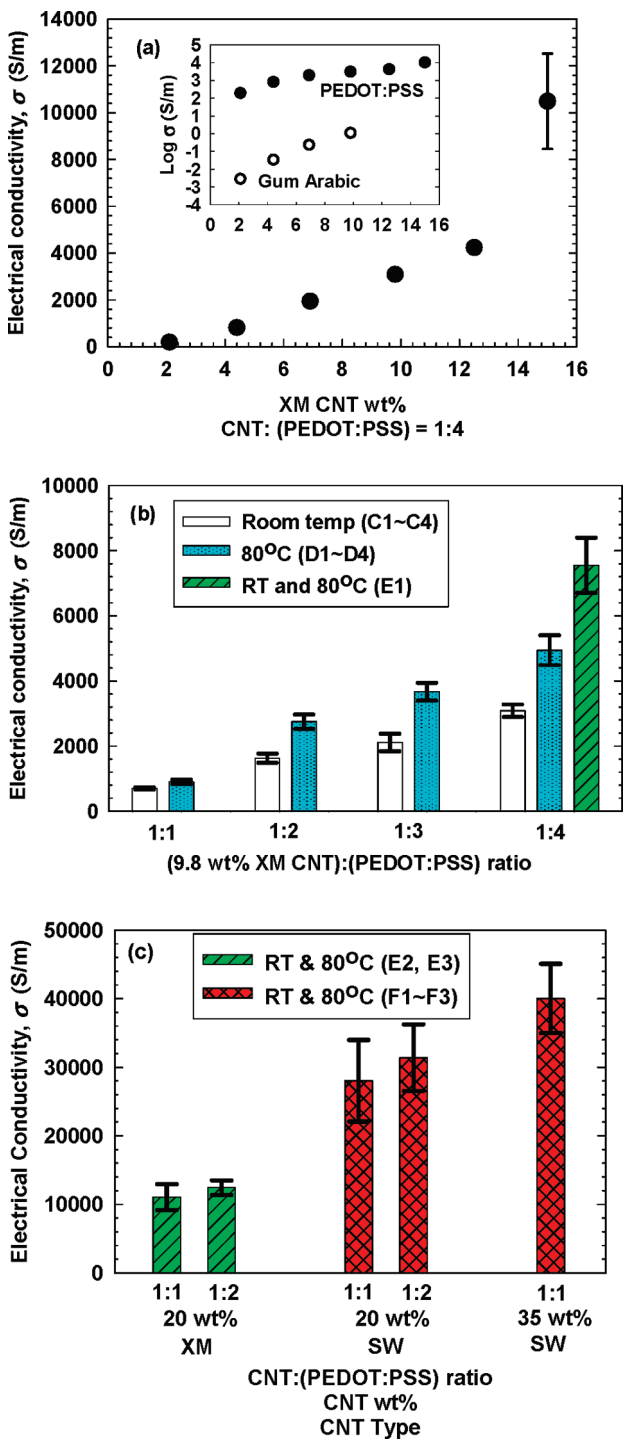


**Figure 4.** (a) Electrical conductivities of 2.1, 4.4, 6.9, 9.8, 12.5, or 15 wt % CNT composites (samples A1–A6, respectively) at room temperature. To compare the role of the stabilizer, electrical conductivity of samples B1–B4 (GA stabilizer, hollow circles) is plotted in the linear–log scale inset with those of samples A1–A6 (PEDOT:PSS stabilizer, filled circles). (b) Electrical conductivities of the composites with 1:1, 1:2, 1:3, or 1:4 ratio between CNT and PEDOT:PSS (samples C1–C4, D1–D4, and E1) at room temperature. CNT concentration is fixed to 9.8 wt %. (c) Electrical conductivities of the composites with XM-CNT (20 wt %) or SWCNT (20 or 35 wt %) and 1:1 or 1:2 ratio between CNT and PEDOT:PSS (samples E2, E3, and F1–F3) at room temperature.

at an elevated temperature. With reduced modulus, the emulsion particles can more effectively deform and

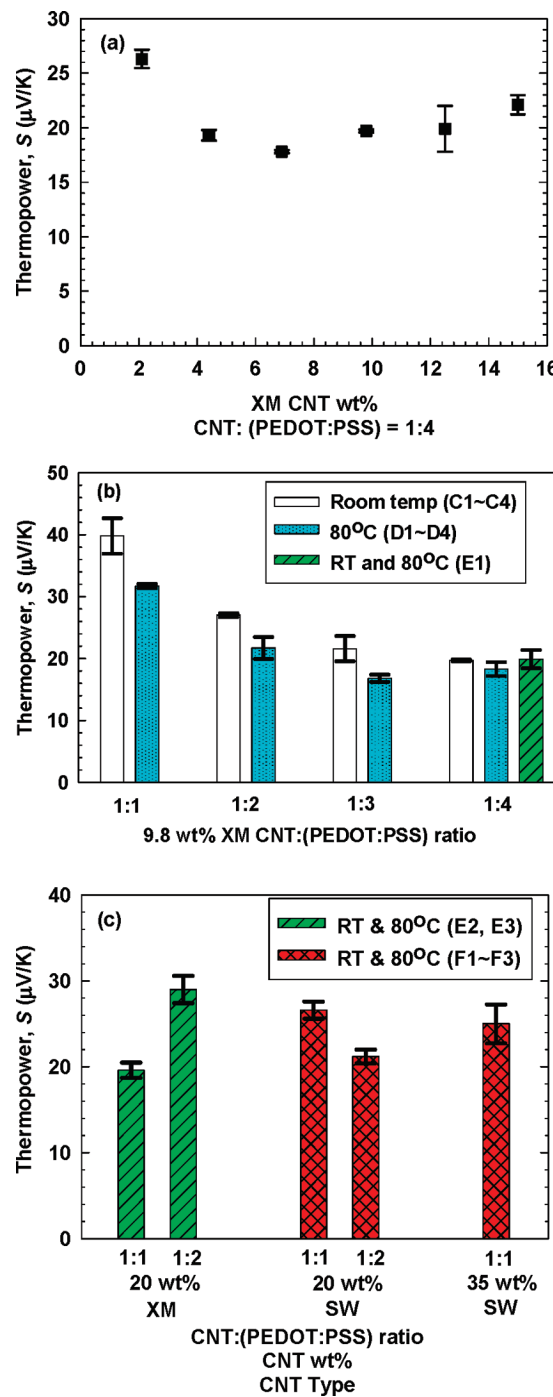
fill the gaps between CNTs. For the mixed drying temperature (samples E and F), composites were allowed to dry at room temperature typically for ~36 h, and then heated to 80 °C for around 6 additional hours. As shown in Figure 3e for sample E1, the microstructure of the composite dried at this mixed temperature is similar to that of the composites dried at only 80 °C.

Figure 4a shows the electrical conductivity of 2.2, 4.4, 6.9, 9.8, 12.5, and 15 wt % CNT filled composites with 1:4 weight ratio of CNTs to PEDOT:PSS dried at room temperature (samples A1–A6). As the CNT concentration increases, the electrical conductivity is dramatically enhanced. A conductivity of ~11700 S/m at 15 wt % CNT loading (CNT: (PEDOT:PSS)=1:4) is comparable to that of the composite (sample E2, ~12400 S/m) prepared with 20 wt % CNT concentration and 1:2 ratio of CNT to PEDOT:PSS. Note that electrical conductivities of  $10^{-2}$ – $10^1$  S/m are typically observed in traditional nanotube-filled polymer composites with similar concentrations.<sup>13,32,33</sup> On the other hand, when the composite was stabilized with GA (samples B1–B4), electrical conductivity was lowered by a factor of  $10^4$  or more, as indicated in the linear–log scale inset of Figure 4a. PEDOT:PSS is believed to create better electrically connected bridges between tubes than those of insulating GA. This is a strong indication that electronic properties can be manipulated by altering junctions between nanoparticles. For better thermoelectric energy conversion, it is necessary to pass as many electrons as possible across the junctions for high electrical conductivity, while low energy electron transport is deterred at the junctions for a large thermopower.

To study the role of PEDOT:PSS, the concentration of PEDOT:PSS was varied with fixed CNT concentrations (9.8 and 20 wt %). Furthermore, the influence of the drying condition and filler type on transport properties was investigated. Figure 4b shows the electrical conductivities of composites with 1:1, 1:2, 1:3, or 1:4 weight ratio of 9.8 wt % XM-CNTs to PEDOT:PSS. These composites were dried at room temperature, 80 °C, or combination of room temperature and 80 °C, as described earlier. As the PEDOT:PSS ratio is increased, electrical conductivity is consistently enhanced irrespective of the drying condition. PEDOT:PSS is electrically conductive, resulting in electrically less resistive tube–tube junctions and self-made electron pathways. Increasing the PEDOT:PSS loading results in a large number of electrically bridged junctions until the conductivity becomes similar to that of completely covered tubes. The electrical conductivity of the sample dried at 80 °C was increased as much as 1.5–2 times compared to the sample dried at room temperature because this elevated temperature often tightens nanoparticle networks.<sup>34</sup> In addition, the composites dried at room temperature show a significant level of porosity due to intertube gaps. These pores can be eliminated when the drying temperature is raised to 80 °C because the

emulsion particles effectively deform around CNTs and fill the gaps between them. The enhancement in electrical conductivity from the mixed drying condition comes from a slow drying process (*e.g.*, more time for segregation) during the initial stage of the segregated network formation. Additionally, 20 wt % CNT dispersed by 40 wt % PEDOT:PSS (total electrically conductive solids are 60 wt %) was synthesized with the mixed drying condition. Electrical conductivity was increased to a value similar to sample A6 whose CNT concentration and electrically conductive solid content were 15 and 75 wt %, respectively (Figure 4c). When the XM-CNT (20 wt %) was replaced by SWCNT, electrical conductivity increased approximately three times, as shown in Figure 4c. At 35 wt % CNT loading, the composite reaches ~40000 S/m, which is among the highest electrical conductivities ever reported for carbon-based composites.

Despite the large increase in electrical conductivity by raising CNT loading, thermopower remains more or less the same, ranging from 15 to 30  $\mu\text{V/K}$  for samples A1–A6, as shown in Figure 5a. These thermopower values are smaller than those in our earlier report (40–60  $\mu\text{V/K}$ )<sup>6</sup> due to the high loading of PEDOT:PSS that has a small thermopower (~10  $\mu\text{V/K}$ )<sup>27,35</sup>. Thermopower of a PEDOT:PSS composite without CNTs (30 wt % PEDOT:PSS and 70 wt % Airflex) was measured to be 17  $\mu\text{V/K}$  with electrical conductivity of 1050 S/m, which is close to the lower bound of the thermopower of the 1:4 ratio composites (samples A2–A5). The low thermopower of PEDOT:PSS appears to be largely responsible for the decrease when more PEDOT:PSS was added, as shown in Figure 5b. Composites dried at 80 °C (samples D1–D4) exhibited thermopowers lower than those of room-temperature dried samples (samples C1–C4). Interestingly, the thermopower of Sample E1, dried at room temperature and subsequently 80 °C, was not considerably diminished, despite a large increase in its electrical conductivity. This seeming contradiction is believed to be due to the combination of a better segregated network and improved DMSO doping. In general, emulsion particles that are more rigid at lower temperature tend to segregate CNTs better than ones that become soft at an elevated temperature, while DMSO dopes more effectively at a temperature higher than room temperature. Larger electrical conductivity and thermopower from 20 wt % XM-CNT (sample E3) than those of sample E2 are likely to be from better dispersion with larger PEDOT:PSS concentration upon relatively high CNT concentration (Figures 4c and 5c). Thermopowers of the samples made of SWCNTs (samples F1–F3) are more or less the same as those of XM-CNT despite high electrical conductivity. Power factors ( $S^2\sigma$ ) of these composites are plotted in Figure 6. Figure 6a suggests that the power factor can be exponentially increased by incorporating more CNTs into the matrix. According to the results in Figure 6b, at a fixed 9.8 wt % CNT concentration, higher PEDOT:PSS loading is better due to higher electrical conductivity. For the



**Figure 5.** (a) Thermopowers of 2.1, 4.4, 6.9, 9.8, 12.5, or 15 wt % CNT composites (samples A1–A6, respectively) at room temperature. (b) Thermopowers of the composites with 1:1, 1:2, 1:3, or 1:4 ratio between CNT and PEDOT:PSS (samples C1–C4, D1–D4, and E1) at room temperature. (c) Thermopowers of the composites with XM-CNT (20 wt %) or SWCNT (20 or 35 wt %) and 1:1 or 1:2 ratio between CNT and PEDOT:PSS (samples E2, E3, and F1–F3) at room temperature.

SWCNT composites (samples F1–F3), a decrease in thermopower from higher PEDOT:PSS loading resulted in lower power factor. The highest power factor in the present work was measured to be ~25  $\mu\text{W}/(\text{m} \cdot \text{K})^2$  from 35 wt % SWCNT and PEDOT:PSS with the mixed drying temperature.

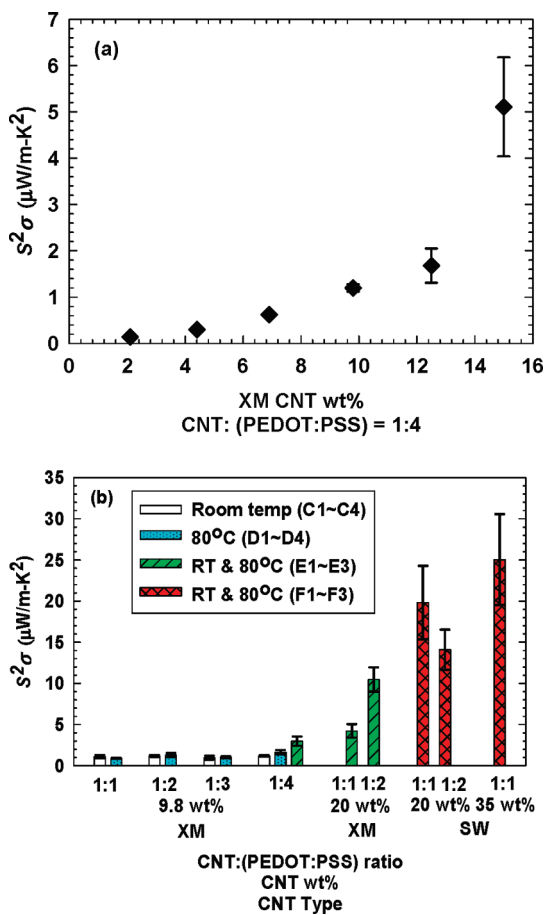


**Figure 6.** (a) Power factors ( $S^2\sigma$ ) of 2.1, 4.4, 6.9, 9.8, 12.5, or 15 wt % CNT composites (samples A1–A6, respectively) at room temperature. (b)  $S^2\sigma$  of the composites with 1:1, 1:2, 1:3, or 1:4 ratio between CNT and PEDOT:PSS composites with the fixed 9.8 wt % CNT concentration (samples C1–C4, D1–D4, and E1) at room temperature.  $S^2\sigma$  of the composites with XM-CNT (20 wt %) or SWCNT (20 or 35 wt %) and 1:1 or 1:2 ratio between CNT and PEDOT:PSS (samples E2, E3, and F1–F3) at room temperature are also shown in panel b.

Unlike electrical conductivity, thermal conductivity is relatively insensitive to CNT and PEDOT:PSS concentrations. A small quantity of CNTs may act as impurities in the polymer matrix and suppress thermal conductivity, but the relatively small increase in thermal conductivity, even at high CNT concentration (15 wt %), is different from the behavior of typical bulks. Figure 7(a) shows that thermal conductivity increases about 50% as the CNT concentration is raised from 2 to 15 wt % with 1:4 ratio of CNT to PEDOT:PSS. Conversely, thermal conductivity decreases about 13% when PEDOT:PSS concentration is increased with respect to the fixed 9.8 wt % CNT concentration, as shown in Figure 7b. Thermal conductivity ( $k$ ) of a composite can be described by a parallel thermal resistor model as

$$k = k_m V_m + k_f V_f \quad (2)$$

where  $k_m$  and  $k_f$  are thermal conductivities of a matrix and a filler, and  $V_i$  represents the volume “fraction” of the indexed ( $i$ ) material, m (matrix), and f (filler) (i.e., the vol-

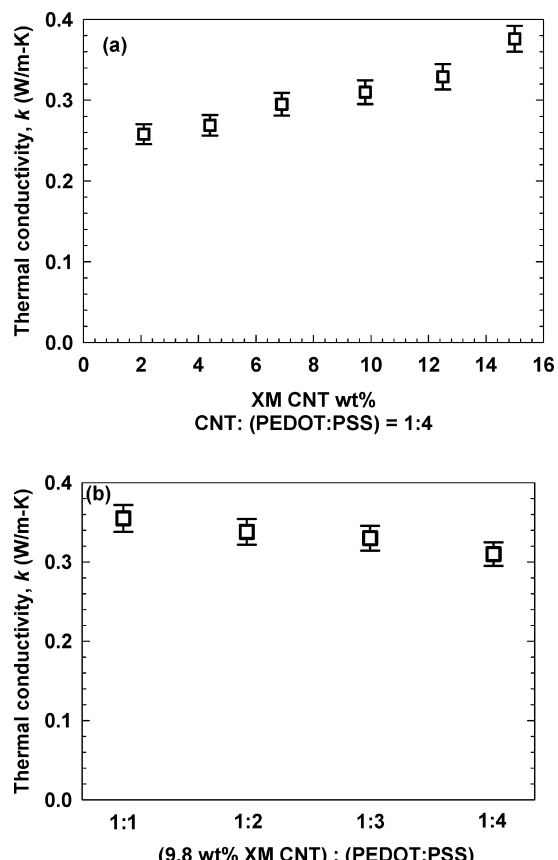


**Figure 7.** (a) Thermal conductivities of 2.1, 4.4, 6.9, 9.8, 12.5, or 15 wt % CNT composites (samples A1–A6, respectively) at room temperature. (b) Thermal conductivities of the composites with 1:1, 1:2, 1:3, or 1:4 ratio between CNT and PE-DOT:PSS (samples C1–C4) at room temperature. CNT concentration is fixed to 9.8 wt %.

ume of the indexed material divided by total volume). Note that the weight percent is close to the volume percent in this study (densities of the polymer matrix, CNT, and PEDOT:PSS are similar,  $\sim 1.2$ ,  $\sim 1.3$ , and  $1 \text{ g/cm}^3$ , respectively).<sup>6,7,31</sup> The thermal conductivity of the matrix ( $k_m$ ) is lower than that of CNT ( $k_f$ ), yielding an increase of composite thermal conductivity upon higher CNT loading. The measured thermal conductivity of the composite, however, is much smaller than an estimated value, considering thermal conductivities of a typical polymer ( $k_m$ ) and CNT ( $k_f$ ) are  $\sim 0.2$  and  $\sim 1000 \text{ W}/(\text{m} \cdot \text{K})$ ,<sup>6,36–38</sup> respectively. For instance, at 15 wt % CNT, thermal conductivity is predicted to be  $\sim 170 \text{ W}/(\text{m} \cdot \text{K})$ , as compared to an actual value of  $\sim 0.36 \text{ W}/(\text{m} \cdot \text{K})$ . This would be due to thermally poor tube–tube connections, making  $k_f'$  different from the intrinsic thermal conductivity ( $k_f$ ) of CNTs.<sup>39,40</sup> In other words,  $k_f'$  is much smaller than  $k_f$  in these composites ( $k_f' \ll k_f$ ). The suppression in thermal conductivity at higher PEDOT:PSS loadings would suggest that many of tube–tube junctions are connected by PEDOT:PSS, making less favorable paths for thermal energy transport. Polymers like PEDOT:PSS have different vibrational spectra from those of CNTs, impeding phonon transport across CNT–(PEDOT:PSS)–CNT interfaces. As a result, the

higher loading of PEDOT:PSS interferes with the phonon transport. Additionally, particle-like PEDOT:PSS embedded in the composite may act as scattering centers for phonons. For the 35 wt % SWCNT composite (sample F3),  $ZT$  is calculated to be  $\sim 0.02$  at 300 K, with an estimated thermal conductivity of  $\sim 0.4$  W/(m · K). This  $ZT$  is at least 1 order of magnitude greater than those of the previous studies with polymer composites<sup>35,41–45</sup> and higher than typical values of bulk semiconductor materials such as silicon ( $ZT \approx 0.01$ <sup>46</sup>).

## CONCLUSIONS

A series of segregated-network CNT-polymer composites were prepared, and their thermoelectric properties (electrical conductivity, thermopower, and thermal conductivity) and microstructure were characterized. Composites were made with two different nanotubes (XM-CNT and SWCNT) and stabilizers (PEDOT:PSS and GA) and four different ratios of CNT to PEDOT:PSS, dried at room temperature or/and 80 °C. This study revealed the influence of the most important composite parameters—CNT type and concentration, stabilizer, and drying temperature—on thermoelectric properties. PEDOT:PSS attaches to CNTs and presumably bridges tube–tube junctions. This electrically conducting PE-

DOT:PSS helps electrons (*i.e.*, holes) to travel more efficiently in the composites, resulting in high electrical conductivity. Thermal transport across the tube–tube junctions, however, is impeded due to mismatches in vibrational spectra between CNT and PEDOT:PSS. This behavior is ideal for developing better thermoelectric materials. Thermal conductivities of various composites, with 2–15 wt % CNT concentration and 1:1–1:4 ratios of CNT to PEDOT:PSS, were within those of typical polymeric materials (0.2–0.4 W/(m · K)). On the other hand, with 35 wt % CNT, electrical conductivity was raised to  $\sim 40000$  S/m, while thermopower and thermal conductivity remained relatively constant. This electrical conductivity is much greater than those of typical polymer composites containing CNTs. Unlike bulk materials, these composites have thermally disconnected, but electrically connected junctions between conducting particles. The best composites in the present work contains 35 wt % SWCNT and 35 wt % PEDOT:PSS, dried at room temperature and subsequently at 80 °C. This recipe achieved a  $ZT$  of  $\sim 0.02$ , but may be further increased by using an intrinsically conductive polymer matrix, adding filler materials with high thermopower and electrical conductivity, and varying filler concentrations.

## METHODS

**Materials.** A vinyl acetate–ethylene copolymer emulsion (Airflex 401 made by Air Products, Inc.) served as a matrix material of the composite for this study. This latex contains 55.2 wt % solids in water and exhibits a  $T_g$  of  $\sim -15$  °C when dried into a film. Prior to drying, the Airflex emulsion exists as an aqueous suspension of polydispersed polymer particles that are 0.14–3.5  $\mu\text{m}$  in diameter (an average diameter of  $\sim 650$  nm). XM-grade CNTs (XM-CNTs) and purified single-wall carbon nanotubes (SWCNTs) were purchased from Carbon Nanotechnologies. XM-CNTs are a mixture of metallic and semiconducting single-, double-, and triple-walled CNTs. Gum arabic (GA) purchased from Sigma-Aldrich was used as a stabilizer for the nanotubes in water. The other stabilizer, poly(3,4-ethylenedioxythiophene) doped with poly(styrenesulfonate) (PEDOT:PSS), was purchased from H. C. Starck (CLEVIOS P for samples A, B, C, D, and E1 or CLEVIOS PH 500 for samples E2 and F). PEDOT:PSS exists as a suspension containing 1.3 wt % solids (0.5 wt % PEDOT and 0.8 wt % PSS) in water.

**Composite Preparation.** To increase electrical conductivity, PEDOT:PSS was mixed with DMSO (Sigma-Aldrich, Co.) for 2 h at room temperature. Next, CNTs were combined with either the PEDOT:PSS suspension or 2 wt % GA in water by sonication with a VirTis Virsonic 100 ultrasonic cell disrupter (SP industries, Inc.) for  $\sim 15$  min at  $\sim 50$  W. The Airflex emulsion and deionized water were then added to the CNT/stabilizer mixtures to obtain an aqueous precomposite mixture of 2.5 wt % total solids (except for the composites with 20 and 35 wt % CNT concentrations, whose total solids were  $\sim 1.5$  wt % or less to reduce viscosity) followed by several minute sonication. Total solid weight including water is typically 20 g. The pH value of the composite mixtures were then adjusted to 2–2.9 because carbon nanotubes are well dispersed at this pH level.<sup>47</sup> All sample concentrations are based upon the total dry weight of the composite, which includes CNTs, emulsion solids, GA, and PEDOT:PSS. Solid composites were made by drying aqueous mixtures in a 26 cm<sup>2</sup> plastic mold for  $\sim 5$  days under ambient conditions and then for 24 h in a vacuum desiccator prior to testing to completely remove re-

sidual water. Samples D1–D4 were dried for  $\sim 6$  h in 80 °C and then for 24 h in a vacuum desiccator at room temperature. In the case of combination drying (samples E and F), composites were dried for  $\sim 36$  h under ambient conditions and then for  $\sim 6$  h in 80 °C and then for 24 h in a vacuum desiccator at room temperature. The thicknesses of the tested composites were 0.07–0.13 mm.

**Composite Characterization.** Electrical conductivity and thermopower were measured with a homemade shielded four-point probe apparatus with a Keithley 2000 Multimeter (Cleveland, OH) and a GW PPS-3635 power supply (Good Will Instrument Co., LTD) in conjunction with Labview (National Instruments, Austin, TX). Composite microstructures were imaged with an FEI Quanta 600 field-emission scanning electron microscope (Hillsboro, OR). Films were soaked in liquid nitrogen and fractured by hand and the surfaces were sputter-coated with 4 nm of platinum prior to SEM imaging. For electrical conductivity and thermopower measurements, samples were cut into pieces of a rectangular shape (typically ca. 30 mm  $\times$  7 mm) and suspended by using a thermal paste between two thermoelectric devices (typically  $\sim 15$  mm apart) used for creating temperature difference. Electrical conductance was measured by using a current–voltage ( $I$ – $V$ ) sweeping measurement technique with four-point probes after four metal lines were patterned with a silver paint. For the thermopower measurement, temperature gradients along the long edge of the sample were measured by two T-type thermocouples. The thermoelectric voltages were measured while the temperature gradient was altered. Thermal conductivity was measured along the film thickness direction with a homemade ASTM D5470 standard setup.

**Acknowledgment.** The authors gratefully acknowledge financial support from the US Air Force Office of Scientific Research (Grant No. FA9550-09-1-0609) under the auspices of Dr. Charles Lee, and the Texas Engineering Experiment Station (TEES). Additionally, J.C.G. acknowledges financial support from the National Science Foundation (Grant CMMI 0644055).

## REFERENCES AND NOTES

- Chen, G.; Dresselhaus, M. S.; Dresselhaus, G.; Fleuriol, J. P.; Caillat, T. Recent Developments in Thermoelectric Materials. *Int. Mater. Rev.* **2003**, *48*, 45–66.
- Tritt, T. M.; Boettner, H.; Chen, L. Thermoelectrics: Direct Solar Thermal Energy Conversion. *MRS Bull.* **2008**, *33*, 366–368.
- Majumdar, A. Thermoelectricity in Semiconductor Nanostructures. *Science* **2004**, *303*, 777–778.
- Winder, E. J.; Ellis, A. B.; Lisensky, G. C. Thermoelectric Devices: Solid-State Refrigerators and Electrical Generators in the Classroom. *J. Chem. Educ.* **1996**, *73*, 940–946.
- Rowe, D. M. *CRC Handbook of Thermoelectrics*; CRC Press: Boca Raton, FL, 1995.
- Yu, C.; Kim, Y. S.; Kim, D.; Grunlan, J. C. Thermoelectric Behavior of Segregated-Network Polymer Nanocomposites. *Nano Lett.* **2008**, *8*, 4428–4432.
- Grunlan, J. C.; Kim, Y.-S.; Ziaeef, S.; Wei, X.; Abdel-Magid, B.; Tao, K. Thermal and Mechanical Behavior of Carbon-Nanotube-Filled Latex. *Macromol. Mater. Eng.* **2006**, *291*, 1035–1043.
- Grunlan, J. C.; Gerberich, W. W.; Francis, L. F. Electrical and Mechanical Behavior of Carbon Black-Filled Poly(vinyl acetate) Latex-Based Composites. *Polym. Eng. Sci.* **2001**, *41*, 1947–1962.
- Grossiord, N.; Loos, J.; van, L.; Maryse, L.; C., M.; E., Z. C.; A., K.; Hart, J. High-Conductivity Polymer Nanocomposites Obtained by Tailoring the Characteristics of Carbon Nanotube Fillers. *Adv. Funct. Mater.* **2008**, *18*, 3226–3234.
- Grunlan, J. C.; Mehrabi, A. R.; Bannon, M. V.; Bahr, J. L. Water-Based Single-Walled-Nanotube-Filled Polymer Composite with an Exceptionally Low Percolation Threshold. *Adv. Mater.* **2004**, *16*, 150–153.
- Vaisman, L.; Wagner, H. D.; Marom, G. The Role of Surfactants in Dispersion of Carbon Nanotubes. *Adv. Colloid Interface Sci.* **2006**, *37*–46.
- Bandyopadhyaya, R.; Nativ-Roth, E.; Regev, O.; Yerushalmi-Rozen, R. Stabilization of Individual Carbon Nanotubes in Aqueous Solutions. *Nano Lett.* **2002**, *2*, 25–28.
- Emmanuel, K.; Gehan, A. J. A. Electrical Properties of Single-Wall Carbon Nanotube-Polymer Composite Films. *J. Appl. Phys.* **2006**, *99*, 084302:1–7.
- Hermant, M. C.; Klumperman, B.; Kyrylyuk, A. V.; van der Schoot, P.; Koning, C. E. Lowering the Percolation Threshold of Single-Walled Carbon Nanotubes Using Polystyrene/poly(3,4-ethylenedioxothiophene):Poly(styrene sulfonate) Blends. *Soft Matter* **2009**, *5*, 878–885.
- Tummala, N. R.; Striolo, A. SDS Surfactants on Carbon Nanotubes: Aggregate Morphology. *ACS Nano* **2009**, *3*, 595–602.
- Grossiord, N.; Loos, J.; Regev, O.; Koning, C. E. Toolbox for Dispersing Carbon Nanotubes into Polymers To Get Conductive Nanocomposites. *Chem. Mater.* **2006**, *18*, 1089–1099.
- Wang, H.; Zhou, W.; Ho, D. L.; Winey, K. I.; Fischer, J. E.; Glinka, C. J.; Hobbie, E. K. Dispersing Single-Walled Carbon Nanotubes with Surfactants: A Small Angle Neutron Scattering Study. *Nano Lett.* **2004**, *4*, 1789–1793.
- Moore, V. C.; Strano, M. S.; Haroz, E. H.; Hauge, R. H.; Smalley, R. E. Individually Suspended Single-Walled Carbon Nanotubes in Various Surfactants. *Nano Lett.* **2003**, *3*, 1379–1382.
- Grunlan, J. C.; Liu, L.; Regev, O. Weak Polyelectrolyte Control of Carbon Nanotube Dispersion in Water. *J. Colloid Interface Sci.* **2008**, *317*, 346–349.
- Dror, Y.; Pyckhout-Hintzen, W.; Cohen, Y. Conformation of Polymers Dispersing Single-Walled Carbon Nanotubes in Water: A Small-Angle Neutron Scattering Study. *Macromolecules* **2005**, *38*, 7828–7836.
- Ouyang, J.; Chu, C. W.; Chen, F. C.; Xu, Q.; Yang, Y. High-Conductivity Poly(3,4-ethylenedioxothiophene):Poly(styrene sulfonate) Film and Its Application in Polymer Optoelectronic Devices. *Adv. Funct. Mater.* **2005**, *15*, 203–208.
- Ouyang, J.; Xu, Q.; Chu, C.-W.; Yang, Y.; Li, G.; Shinar, J. On the Mechanism of Conductivity Enhancement in Poly(3,4-ethylenedioxothiophene):Poly(styrene sulfonate) Film through Solvent Treatment. *Polymer* **2004**, *45*, 8443–8450.
- Haggenmueller, R.; Rahatekar, S. S.; Fagan, J. A.; Chun, J.; Becker, M. L.; Naik, R. R.; Krauss, T.; Carlson, L.; Kadla, J. F.; Trulove, P. C.; et al. Comparison of the Quality of Aqueous Dispersions of Single Wall Carbon Nanotubes Using Surfactants and Biomolecules. *Langmuir* **2008**, *24*, 5070–5078.
- Zheng, M.; Jagota, A.; Semke, E. D.; Diner, B. A.; Robert, S. McLean; Lustig, S. R.; Richardson, R. E.; Tassi, N. G. DNA-Assisted Dispersion and Separation of Carbon Nanotubes. *Nat. Mater.* **2003**, *2*, 338–342.
- Tsai, Y.-C.; Chiu, C.-C.; Tsai, M.-C.; Wu, J.-Y.; Tzu-Fan Tseng; Wu, T.-M.; Hsu, S.-F. Dispersion of Carbon Nanotubes in Low pH Aqueous Solutions by Means of Alumina-Coated Silica Nanoparticles. *Carbon* **2007**, *45*, 2823–2827.
- Liu, L.; Grunlan, J. C. Clay Assisted Dispersion of Carbon Nanotubes in Conductive Epoxy Nanocomposites. *Adv. Funct. Mater.* **2007**, *17*, 2343–2348.
- Kim, J. Y.; Jung, J. H.; Lee, D. E.; Joo, J. Enhancement of Electrical Conductivity of Poly(3,4-ethylenedioxothiophene)/poly(4-styrenesulfonate) by a Change of Solvents. *Synth. Met.* **2002**, *126*, 311–316.
- Joseph; Grodzinski, J. Electronically Conductive Polymers. *Polym. Advan. Technol.* **2002**, *13*, 615–625.
- Kirchmeyer, S.; Reuter, K. Scientific Importance, Properties and Growing Applications of Poly(3,4-ethylenedioxothiophene). *J. Mater. Chem.* **2005**, *15*, 2077–2088.
- De, S.; Lyons, P. E.; Sorel, S.; Doherty, E. M.; King, P. J.; Blau, W. J.; Nirmalraj, P. N.; Boland, J. J.; Scardaci, V.; Joimel, J.; Coleman, J. N. Transparent, Flexible, and Highly Conductive Thin Films Based on Polymer–Nanotube Composites. *ACS Nano* **2009**, *3*, 714–720.
- Clevios P Formulation Guide*; H.C. Starck Co. Newton, MA, 2008.
- Das, N. C.; Liu, Y.; Yang, K.; Peng, W.; Maiti, S.; Wang, H. Single-Walled Carbon Nanotube/Poly(methylmethacrylate) Composites for Electromagnetic Interference Shielding. *Poly. Eng. Sci.* **2009**, *49*, 1461–1669.
- Zhu, D.; Bin, Y.; Matsuo, M. Electrical Conducting Behaviors in Polymeric Composites with Carbonaceous Fillers. *J. Polym. Sci. B* **2007**, *45*, 1037–1044.
- Kim, Y. S.; Wright, J. B.; Grunlan, J. C. Influence of Polymer Modulus on the Percolation Threshold of Latex-Based Composites. *Polymer* **2008**, *49*, 570–578.
- Chang, K.-C.; Jeng, M.-S.; Yang, C.-C.; Chou, Y.-W.; Wu, S.-K.; Thomas, M. A.; Peng, Y.-C. The Thermoelectric Performance of Poly(3,4-ethylenedioxothiophene)/Poly(4-styrenesulfonate) Thin Films. *J. Electron. Mater.* **2009**, *38*, 1182–1188.
- Yu, C.; Shi, L.; Yao, Z.; Li, D.; Majumdar, A. Thermal Conductance and Thermopower of an Individual Single-Wall Carbon Nanotube. *Nano Lett.* **2005**, *5*, 1842–1846.
- Berber, S.; Kwon, Y. K.; Tománek, D. Unusually High Thermal Conductivity of Carbon Nanotubes. *Phys. Rev. Lett.* **2000**, *84*, 4613–4616.
- Che, J. W.; Çağın, T.; Goddard, W. A. Thermal Conductivity of Carbon Nanotubes. *Nanotechnology* **2000**, *11*, 65–69.
- Yu, C. Nanomaterials Characterization and Bio-chemical Sensing Using Microfabricated Devices. Ph.D. Thesis. University of Texas at Austin, Texas, 2004.
- Shi, L.; Li, D.; Yu, C.; Jang, W. Y.; Kim, D.; Yao, Z.; Kim, P.; Majumdar, A. Measuring Thermal and Thermoelectric Properties of One-Dimensional Nanostructures Using a Microfabricated Device. *J. Heat Transfer* **2003**, *125*, 881–888.
- Hostler, S. R.; Kaul, P.; Day, K.; Qu, V.; Cullen, C.; Abramson, A. R. Thermal and Electrical Characterization of Nanocomposites for Thermoelectrics. *ITHERM '06 10th Intersoc. Conf.* **2006**, 1400–1405.

42. Yoshino, K.; Morita, S.; Yin, X. H.; Onoda, M. Electrical Property of Polypyrrole-Insulating Polymer Composite. *Synth. Met.* **1993**, *55–57*, 3562–3565.
43. Joussemae, V.; Morsli, M.; Bonnet, A.; Tesson, O.; Lefrant, S. Electrical Properties of Polyaniline–Polystyrene Blends above the Percolation Threshold. *J. Appl. Polym. Sci.* **1998**, *67*, 1205–1208.
44. Anilkumar, K. R.; Parveen, A.; Badiger, G. R.; Prasad, M. V. N. A. Thermoelectric Power Factor for Polyaniline/Molybdenum Trioxide Composites. *Ferroelectrics* **2009**, *386*, 88–93.
45. Levesque, I.; Gao, X.; Klug, D. D.; Tse, J. S.; Ratcliffe, C. I.; Leclerc, M. Highly Soluble Poly(2,7-carbazolevinylene) for Thermoelectrical Applications: From Theory to Experiment. *React. Funct. Polym.* **2005**, *65*, 23–36.
46. Weber, L.; Gmelin, E. Transport Properties of Silicon. *Appl. Phys. A* **1991**, *53*, 136–140.
47. Grunlan, J. C.; Liu, L.; Kim, Y. S. Tunable Single-Walled Carbon Nanotube Microstructure in the Liquid and Solid States Using Poly(acrylic acid). *Nano Lett.* **2006**, *6*, 911–915.